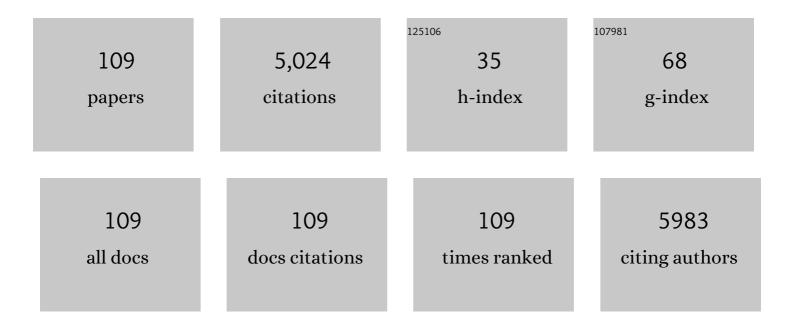
Liang-Liang Li

List of Publications by Year in descending order

Source: https://exaly.com/author-pdf/1345199/publications.pdf Version: 2024-02-01



#	Article	IF	CITATIONS
1	Composite Cathodes with Succinonitrileâ€Based Ionic Conductors for Longâ€Cycleâ€Life Solidâ€State Lithium Metal Batteries. Batteries and Supercaps, 2022, 5, .	2.4	3
2	A Valence Gradient Protective Layer for Dendriteâ€Free and Highly Stable Lithium Metal Anodes. Advanced Energy Materials, 2022, 12, .	10.2	26
3	Significantly improved interface between PVDF-based polymer electrolyte and lithium metal via thermal-electrochemical treatment. Energy Storage Materials, 2022, 46, 452-460.	9.5	21
4	Balancing oxygen evolution reaction and oxygen reduction reaction processes in Li–O2 batteries through tuning the bond distances of RuO2. Composites Part B: Engineering, 2022, 234, 109727.	5.9	5
5	A Cross-Linked Poly(Ethylene Oxide)-Based Electrolyte for All-Solid-State Lithium Metal Batteries With Long Cycling Stability. Frontiers in Materials, 2022, 9, .	1.2	8
6	Super Longâ€Cycling Allâ€5olidâ€5tate Battery with Thin Li ₆ PS ₅ Clâ€Based Electrolyte. Advanced Energy Materials, 2022, 12, .	10.2	58
7	Ion–Dipole Interaction Regulation Enables Highâ€Performance Singleâ€Ion Polymer Conductors for Solidâ€5tate Batteries. Advanced Materials, 2022, 34, .	11.1	49
8	Effects of Molecular Weight on the Electrochemical Properties of Poly(vinylidene difluoride)-Based Polymer Electrolytes. ACS Applied Materials & Interfaces, 2022, 14, 32075-32083.	4.0	17
9	A volatile redox mediator boosts the long-cycle performance of lithium-oxygen batteries. Energy Storage Materials, 2021, 38, 571-580.	9.5	14
10	Lithium Argyrodite as Solid Electrolyte and Cathode Precursor for Solidâ€ S tate Batteries with Long Cycle Life. Advanced Energy Materials, 2021, 11, 2101370.	10.2	56
11	Synthesis of polycrystalline boron nitride nanotubes with Lead(II) oxide and Iron(III) nitrate nonahydrate as promoters. Physica E: Low-Dimensional Systems and Nanostructures, 2021, 133, 114788.	1.3	1
12	Strategies to suppress the shuttle effect of redox mediators in lithium-oxygen batteries. Journal of Energy Chemistry, 2021, 60, 135-149.	7.1	12
13	Polymer electrolytes and interfaces in solid-state lithium metal batteries. Materials Today, 2021, 51, 449-474.	8.3	161
14	High-Performance Flexible Transparent Conductive Films Enabled by a Commonly Used Antireflection Layer. ACS Applied Materials & Interfaces, 2021, 13, 2979-2987.	4.0	8
15	Boron nitride/agarose hydrogel composites with high thermal conductivities. Rare Metals, 2020, 39, 375-382.	3.6	17
16	Boosting thermoelectric performance by in situ growth of metal organic framework on carbon nanotube and subsequent annealing. Carbon, 2020, 157, 324-329.	5.4	31
17	Composition Modulation and Structure Design of Inorganicâ€inâ€Polymer Composite Solid Electrolytes for Advanced Lithium Batteries. Small, 2020, 16, e1902813.	5.2	87
18	Free-standing sulfide/polymer composite solid electrolyte membranes with high conductance for all-solid-state lithium batteries. Energy Storage Materials, 2020, 25, 145-153.	9.5	85

#	Article	IF	CITATIONS
19	Rheological Behavior and Thermal Conductivities of Emulsion-Based Thermal Pastes. Journal of Electronic Materials, 2020, 49, 2100-2109.	1.0	3
20	High-conductivity free-standing Li6PS5Cl/poly(vinylidene difluoride) composite solid electrolyte membranes for lithium-ion batteries. Journal of Materiomics, 2020, 6, 70-76.	2.8	51
21	Conductive gel composite cathodes with high mass loading of active oxides for high-performance solid-state lithium metal batteries. Solid State Ionics, 2020, 345, 115196.	1.3	4
22	Organic–Organic Composite Electrolyte Enables Ultralong Cycle Life in Solid-State Lithium Metal Batteries. ACS Applied Materials & Interfaces, 2020, 12, 24837-24844.	4.0	55
23	High Cycling Stability for Solidâ€State Li Metal Batteries via Regulating Solvation Effect in Poly(Vinylidene Fluoride)â€Based Electrolytes. Batteries and Supercaps, 2020, 3, 876-883.	2.4	84
24	Response to Comment on "Selfâ€Suppression of Lithium Dendrite in Allâ€Solidâ€State Lithium Metal Batteries with Poly(vinylidene difluoride)â€Based Solid Electrolytes― Advanced Materials, 2020, 32, e2000026.	11.1	40
25	Oxygen- and dendrite-resistant ultra-dry polymer electrolytes for solid-state Li–O2 batteries. Energy Storage Materials, 2020, 27, 244-251.	9.5	45
26	High-performance Li ₆ PS ₅ Cl-based all-solid-state lithium-ion batteries. Journal of Materials Chemistry A, 2019, 7, 18612-18618.	5.2	40
27	Development of integrated two-stage thermoelectric generators for large temperature difference. Science China Technological Sciences, 2019, 62, 1596-1604.	2.0	23
28	Experiments and modeling on thermoelectric power generators used for waste heat recovery from hot water pipes. Energy Procedia, 2019, 158, 1052-1058.	1.8	8
29	Ultralow thermal conductance of the van der Waals interface between organic nanoribbons. Materials Today Physics, 2019, 11, 100139.	2.9	25
30	An in Situ-Formed Mosaic Li ₇ Sn ₃ /LiF Interface Layer for High-Rate and Long-Life Garnet-Based Lithium Metal Batteries. ACS Applied Materials & Interfaces, 2019, 11, 34939-34947.	4.0	66
31	Phase-separation-driven formation of Nickel–Cobalt oxide nanotubes as high-capacity anode materials for lithium-ion batteries. Materials Research Letters, 2019, 7, 368-375.	4.1	3
32	Self‣uppression of Lithium Dendrite in All‣olid‣tate Lithium Metal Batteries with Poly(vinylidene) Tj ETC	2q0 0.0 rgB 11.1	BT /Qygrlock 1
33	Dependence of shear strength of Sn–3.8Ag–0.7Cu/Co–P solder joints on the P content of Co–P metallization. Journal of Materials Science: Materials in Electronics, 2019, 30, 5249-5256.	1.1	4
34	Chapter 5. Properties and Applications of Layered Thermoelectric Materials. RSC Smart Materials, 2019, , 129-164.	0.1	0
35	High Capacity and Superior Cyclic Performances of All-Solid-State Lithium Batteries Enabled by a Glass–Ceramics Solo. ACS Applied Materials & Interfaces, 2018, 10, 10029-10035.	4.0	37

Thermoelectric and mechanical properties of PLA/BiO·5Sb1·5Te3 composite wires used for 3D printing. 3.8 47 Composites Science and Technology, 2018, 157, 1-9.

#	Article	IF	CITATIONS
37	Single-crystalline 2D erucamide with low friction and enhanced thermal conductivity. Colloids and Surfaces A: Physicochemical and Engineering Aspects, 2018, 540, 29-35.	2.3	11
38	Microdiamond/PLA composites with enhanced thermal conductivity through improving filler/matrix interface compatibility. Diamond and Related Materials, 2018, 81, 161-167.	1.8	22
39	Pressurized calcium looping in the presence of steam in a spout-fluidized-bed reactor with DFT analysis. Fuel Processing Technology, 2018, 169, 24-41.	3.7	32
40	Enhanced electrochemical performance of bulk type oxide ceramic lithium batteries enabled by interface modification. Journal of Materials Chemistry A, 2018, 6, 4649-4657.	5.2	98
41	High-performance all-solid-state lithium–sulfur batteries with sulfur/carbon nano-hybrids in a composite cathode. Journal of Materials Chemistry A, 2018, 6, 23345-23356.	5.2	48
42	High-Conductivity Argyrodite Li ₆ PS ₅ Cl Solid Electrolytes Prepared via Optimized Sintering Processes for All-Solid-State Lithium–Sulfur Batteries. ACS Applied Materials & Interfaces, 2018, 10, 42279-42285.	4.0	170
43	Effects of Li6.75La3Zr1.75Ta0.25O12 on chemical and electrochemical properties of polyacrylonitrile-based solid electrolytes. Solid State Ionics, 2018, 327, 32-38.	1.3	55
44	FeVSb-based amorphous films with ultra-low thermal conductivity and high <i>ZT</i> : a potential material for thermoelectric generators. Journal of Materials Chemistry A, 2018, 6, 11435-11445.	5.2	5
45	Micro-thermoelectric generators based on through glass pillars with high output voltage enabled by large temperature difference. Applied Energy, 2018, 225, 600-610.	5.1	46
46	Lithium-Salt-Rich PEO/Li _{0.3} La _{0.557} TiO ₃ Interpenetrating Composite Electrolyte with Three-Dimensional Ceramic Nano-Backbone for All-Solid-State Lithium-Ion Batteries. ACS Applied Materials & Interfaces, 2018, 10, 24791-24798.	4.0	230
47	Giant energy density and high efficiency achieved in bismuth ferrite-based film capacitors via domain engineering. Nature Communications, 2018, 9, 1813.	5.8	408
48	BiFeO ₃ –SrTiO ₃ thin film as a new lead-free relaxor-ferroelectric capacitor with ultrahigh energy storage performance. Journal of Materials Chemistry A, 2017, 5, 5920-5926.	5.2	218
49	The Gadolinium (Gd3+) and Tin (Sn4+) Co-doped BiFeO3 Nanoparticles as New Solar Light Active Photocatalyst. Scientific Reports, 2017, 7, 42493.	1.6	115
50	SeO 2 adsorption on CaO surface: DFT study on the adsorption of a single SeO 2 molecule. Applied Surface Science, 2017, 413, 366-371.	3.1	45
51	Enhanced photocatalytic activity of La ³⁺ and Se ⁴⁺ co-doped bismuth ferrite nanostructures. Journal of Materials Chemistry A, 2017, 5, 11143-11151.	5.2	116
52	SeO 2 adsorption on CaO surface: DFT and experimental study on the adsorption of multiple SeO 2 molecules. Applied Surface Science, 2017, 420, 465-471.	3.1	44
53	All-solid-state lithium battery with high capacity enabled by a new way of composite cathode design. Solid State Ionics, 2017, 310, 44-49.	1.3	12
54	Zerovalent Selenium Adsorption Mechanisms on CaO Surface: DFT Calculation and Experimental Study. Journal of Physical Chemistry A, 2017, 121, 7385-7392.	1.1	15

Liang-Liang Li

#	Article	IF	CITATIONS
55	Synergistic Coupling between Li _{6.75} La ₃ Zr _{1.75} Ta _{0.25} O ₁₂ and Poly(vinylidene fluoride) Induces High Ionic Conductivity, Mechanical Strength, and Thermal Stability of Solid Composite Electrolytes. Journal of the American Chemical Society, 2017, 139, 13779-13785.	6.6	698
56	Liquid Exfoliation Few-Layer SnSe Nanosheets with Tunable Band Gap. Journal of Physical Chemistry C, 2017, 121, 17530-17537.	1.5	75
57	Ferroelectric strain modulation of antiferromagnetic moments in Ni/NiO ferromagnet/antiferromagnet heterostructures. Physical Review B, 2017, 95, .	1.1	17
58	Pb-free silver pastes with SnO-B <inf>2</inf> O <inf>3</inf> glass frits for crystalline silicon solar cells. , 2017, , .		0
59	Embedded Passives. , 2017, , 537-588.		3
60	Pb-free front-contact silver pastes with SnO P2O5 glass frit for crystalline silicon solar cells. Journal of Alloys and Compounds, 2016, 689, 662-668.	2.8	8
61	Density functional theory study on Hg removal mechanisms of Cu-impregnated activated carbon prepared by simplified method. Korean Journal of Chemical Engineering, 2016, 33, 2869-2877.	1.2	4
62	Fabrication and characterization of thermoelectric power generators with segmented legs synthesized by one-step spark plasma sintering. Energy, 2016, 113, 35-43.	4.5	46
63	Glancing angle deposition of Fe triangular nanoprisms consisting of vertically-layered nanoplates. Journal of Crystal Growth, 2016, 451, 113-119.	0.7	2
64	Significantly enhanced shear strength of Sn-Ag-Cu/Co-P ball grid array solder joints by CoSn <inf>3</inf> intermetallic compound. , 2016, , .		2
65	Thermoelectric and mechanical properties of ZnSb/SiC nanocomposites. Journal of Materials Science, 2016, 51, 5271-5280.	1.7	23
66	A First-Principles Theoretical Study on the Thermoelectric Properties of the Compound Cu5AlSn2S8. Journal of Electronic Materials, 2016, 45, 1453-1458.	1.0	6
67	Kinetics of interfacial reaction between Sn-3.0Ag-0.5Cu solder and Co-4.0P or Co-8.0P metallization. , $2015,,$		2
68	Tunable High-Frequency Properties of Co–Ni Ferromagnetic Nanowires Through Composition Modulation. IEEE Transactions on Magnetics, 2015, 51, 1-6.	1.2	1
69	Thermoelectric Properties of Amorphous Zr-Ni-Sn Thin Films Deposited by Magnetron Sputtering. Journal of Electronic Materials, 2015, 44, 1957-1962.	1.0	12
70	Electronic structures and thermoelectric properties of La or Ce-doped Bi2Te3 alloys from first principles calculations. Journal of Physics and Chemistry of Solids, 2015, 85, 239-244.	1.9	11
71	IMC growth and shear strength of Sn–Ag–Cu/Co–P ball grid array solder joints under thermal cycling. Journal of Materials Science: Materials in Electronics, 2015, 26, 962-969.	1.1	26
72	Evaluation of Electroplated Co-P Film as Diffusion Barrier Between In-48Sn Solder and SiC-Dispersed Bi2Te3 Thermoelectric Material. Journal of Electronic Materials, 2015, 44, 2007-2014.	1.0	14

#	Article	IF	CITATIONS
73	Microstructure and morphology of interfacial intermetallic compound CoSn3 in Sn–Pb/Co–P solder joints. Microelectronics Reliability, 2015, 55, 2403-2411.	0.9	10
74	Microwave properties of ferromagnetic nanowire arrays patterned with periodic and quasi-periodic structures. Journal of Applied Physics, 2015, 117, .	1.1	5
75	Effects of silver nanoparticles on the firing behavior of silver paste on crystalline silicon solar cells. Colloids and Surfaces A: Physicochemical and Engineering Aspects, 2015, 466, 132-137.	2.3	26
76	Thermal Resistance Analysis of Sn-Bi Solder Paste Used as Thermal Interface Material for Power Electronics Applications. Journal of Electronic Packaging, Transactions of the ASME, 2014, 136, .	1.2	30
77	Fast Seebeck coefficient measurement based on dynamic method. Review of Scientific Instruments, 2014, 85, 054904.	0.6	21
78	First-principles study on transition metal-doped anatase TiO2. Nanoscale Research Letters, 2014, 9, 46.	3.1	177
79	Thermoelectric properties of Pb-doped bismuth telluride thin films deposited by magnetron sputtering. Journal of Alloys and Compounds, 2014, 590, 362-367.	2.8	52
80	Reliability of Sn-Pb solder joints with Cu and Co-P surface finishes under thermal cycling. , 2014, , .		0
81	Interfacial reaction between Sn–Ag–Cu solder and Co–P films with various microstructures. Acta Materialia, 2013, 61, 4581-4590.	3.8	57
82	Plasmon Absorption of Au-in-CoAl ₂ O ₄ Linear Nanopeapod Chains. Journal of Physical Chemistry C, 2013, 117, 14142-14148.	1.5	20
83	Wettability of Sn-Bi and Sn-Ag-Cu lead-free solder pastes on electroplated Co-P films. , 2013, , .		5
84	Silver-based thermal interface materials with low thermal resistance. , 2012, , .		6
85	Dual-Band Noise Suppressors Based on Co/Au Multilayered Magnetic Nanowires. IEEE Transactions on Magnetics, 2012, 48, 4398-4401.	1.2	9
86	Dependence of interfacial adhesion of Co–P film on its microstructure. Surface and Coatings Technology, 2012, 206, 4822-4827.	2.2	30
87	Phonon thermal conductivity of GaN nanotubes. Journal of Applied Physics, 2012, 112, .	1.1	14
88	Synthesis and Magnetic Anisotropy Analysis of Co/Au Multilayered Nanowires. IEEE Transactions on Magnetics, 2012, 48, 3925-3928.	1.2	4
89	Temperature dependence of the Raman spectra of Bi ₂ Te ₃ and Bi _{0.5} Sb _{1.5} Te ₃ thermoelectric films. Physica Status Solidi - Rapid Research Letters, 2012, 6, 268-270.	1.2	24
90	Silver nanoparticle-based thermal interface materials with ultra-low thermal resistance for power electronics applications. Scripta Materialia, 2012, 66, 931-934.	2.6	126

#	Article	IF	CITATIONS
91	Thermal and insulating properties of epoxy/aluminum nitride composites used for thermal interface material. Journal of Applied Polymer Science, 2012, 124, 669-677.	1.3	111
92	Integrated Microwave Noise Suppressor Fabricated on Magnetic/Dielectric Composite Ceramic Substrate. Additional Conferences (Device Packaging HiTEC HiTEN & CICMT), 2012, 2012, 000208-000215.	0.2	1
93	Viscosity and thermal conductivity of alumina microball/epoxy composites. , 2011, , .		6
94	Synthesis and low-temperature sintering of tin-doped silver nanoparticles. , 2011, , .		0
95	Synthesis and Characterization of Ultrasonic-Assisted Electroplated Co–P Films With Amorphous and Nanocrystalline Structures. IEEE Transactions on Magnetics, 2011, 47, 3799-3802.	1.2	15
96	20 Gigahertz noise suppressor based on ferromagnetic nanowire arrays. , 2011, , .		7
97	Low alkaline solution to deposit electroless Ni-Zn-P film on al pad. , 2010, , .		Ο
98	Numerical simulation on the noise suppression effect of nanogranular magnetic film CoFeHfO on PCB transmission lines. , 2010, , .		1
99	Fabrication and evaluation of microscale thermoelectric modules of Bi ₂ Te ₃ -based alloys. Journal of Micromechanics and Microengineering, 2010, 20, 125031.	1.5	23
100	Dielectric composite material with enhanced thermal conductivity used for electronic packaging. , 2010, , .		4
101	Multi-pulse electrodeposition of soft magnetic thin film Co-P for embedded inductor application. , 2010, , .		1
102	Embedded Passives. , 2009, , 459-502.		1
103	On-package magnetic materials for embedded inductor applications. , 2009, , .		5
104	Small-Resistance and High-Quality-Factor Magnetic Integrated Inductors on PCB. IEEE Transactions on Advanced Packaging, 2009, 32, 780-787.	1.7	24
105	High-frequency responses of granular CoFeHfO and amorphous CoZrTa magnetic materials. Journal of Applied Physics, 2007, 101, 123912.	1.1	25
106	Tensor Nature of Permeability and Its Effects in Inductive Magnetic Devices. IEEE Transactions on Magnetics, 2007, 43, 2373-2375.	1.2	19
107	Package compatibility and substrate dependence of granular soft magnetic material CoFeHfO developed by reactive sputtering. Journal of Applied Physics, 2006, 99, 08M301.	1.1	6
108	Soft magnetic granular material Co–Fe–Hf–O for micromagnetic device applications. Journal of Applied Physics, 2005, 97, 10F907.	1.1	31

#	Article	IF	CITATIONS
109	Firing and Contact Resistivity of Ag ₂ O-Aided Pb-Free Silver Paste for Crystalline Silicon Solar Cells. Materials Science Forum, 0, 847, 123-130.	0.3	1